University of Groningen

Acetone and the precursor ligand acetylacetone

Warneke, Jonas; Van Dorp, Willem F.; Rudolf, Petra; Stano, Michal; Papp, Peter; Matejcik, Stefan; Borrmann, Tobias; Swiderek, Petra

Published in:
PPCP : Physical Chemistry Chemical Physics

DOI:
10.1039/c4cp04239e

IMPORTANT NOTE: You are advised to consult the publisher's version (publisher's PDF) if you wish to cite from it. Please check the document version below.

Document Version
Publisher's PDF, also known as Version of record

Publication date:
2015

Link to publication in University of Groningen/UMCG research database

Citation for published version (APA):
Warneke, J., Van Dorp, W. F., Rudolf, P., Stano, M., Papp, P., Matejcik, S., Borrmann, T., & Swiderek, P. (2015). Acetone and the precursor ligand acetylacetone: distinctly different electron beam induced decomposition? *PPCP : Physical Chemistry Chemical Physics*, *17*(2), 1204-1216. https://doi.org/10.1039/c4cp04239e

Copyright
Other than for strictly personal use, it is not permitted to download or to forward/distribute the text or part of it without the consent of the author(s) and/or copyright holder(s), unless the work is under an open content license (like Creative Commons).

The publication may also be distributed here under the terms of Article 25fa of the Dutch Copyright Act, indicated by the "Taverne" license. More information can be found on the University of Groningen website: https://www.rug.nl/library/open-access/self-archiving-pure/taverne-amendment.

Take-down policy
If you believe that this document breaches copyright please contact us providing details, and we will remove access to the work immediately and investigate your claim.

Downloaded from the University of Groningen/UMCG research database (Pure): http://www.rug.nl/research/portal. For technical reasons the number of authors shown on this cover page is limited to 10 maximum.

Download date: 27-04-2023

PCCP

PAPER

View Article Online
View Journal | View Issue

Published on 14 November 2014. Downloaded by University of Groningen on 5/21/2019 9:45:41 AM.

Cite this: *Phys. Chem. Chem. Phys.*, 2015, **17**, 1204

Acetone and the precursor ligand acetylacetone: distinctly different electron beam induced decomposition?†

Jonas Warneke,*[a] Willem F. Van Dorp,[b] Petra Rudolf,[b] Michal Stano,[c] Peter Papp,[c] Štefan Matejčík,[c] Tobias Borrmann[a] and Petra Swiderek[a]

Received 21st September 2014,
Accepted 13th November 2014

DOI: 10.1039/c4cp04239e

www.rsc.org/pccp

In focused electron beam induced deposition (FEBID) acetylacetone plays a role as a ligand in metal acetylacetonate complexes. As part of a larger effort to understand the chemical processes in FEBID, the electron-induced reactions of acetylacetone were studied both in condensed layers and in the gas phase and compared to those of acetone. X-ray photoelectron spectroscopy (XPS) shows that the electron-induced decomposition of condensed acetone layers yields a non-volatile hydrocarbon residue while electron irradiation of acetylacetone films produces a non-volatile residue that contains not only much larger amounts of carbon but also significant amounts of oxygen. Electron-stimulated desorption (ESD) and thermal desorption spectrometry (TDS) measurements reveal striking differences in the decay kinetics of the layers. In particular, intact acetylacetone suppresses the desorption of volatile products. Gas-phase studies of dissociative electron attachment and electron impact ionization suggest that this effect cannot be traced back to differences in the initial fragmentation reactions of the isolated molecules but is due to subsequent dissociation processes and to an efficient reaction of released methyl radicals with adjacent acetylacetone molecules. These results could explain the incorporation of large amounts of ligand material in deposits fabricated by FEBID processes using acetylacetonate complexes.

1. Introduction

Acetylacetone is used as a ligand in metal organic chemistry. The resulting metal acetylacetonates are volatile compounds that are employed as precursors in chemical vapor deposition (CVD) of metals[1] and have also been utilized in focused electron beam induced deposition (FEBID). FEBID is a technique that produces micro- and nanometer sized deposits by decomposing precursor molecules adsorbed on a surface under a tightly focused high-energy electron beam.[2] In the ideal case, this leads to pure metal structures while the organic ligands decompose into volatile products that are pumped away.[3] In reality, when acetylacetonate complexes are irradiated with electrons, considerable amounts of carbon impurities[2,4] are found in addition to the metal deposits. It has been argued that such precursors are highly stable and that a large number of electrons is thus needed for their decomposition[5] but the sequence of chemical reactions following the initial electron–molecule interaction is still unidentified and the incomplete degradation of acetylacetonates is not understood. Such knowledge is crucial to devise criteria for the development of better FEBID precursors.

Acetone and acetaldehyde efficiently release CO when irradiated with electrons[6,7] and thus appear to decompose easily. The incomplete electron-induced decomposition of acetylacetonate precursors is therefore surprising. While CO formation in acetone under exposure to low-energy electrons has been quantified thoroughly,[7] the hydrocarbon by-products have not been identified. Also, for a more complete picture, particularly with regards to FEBID, products desorbing from the sample must be monitored in addition to the products formed within the film.

Here we present a comparative study of the electron-induced chemistry of acetone and acetylacetone (molecular structures shown in Fig. 1). Our goal is to obtain insight into the electron-induced chemistry of acetylacetone and to reveal whether the incomplete decomposition of metal acetylacetonates is related to an inherent structural property of the ligand. At and below room temperature acetylacetone predominantly prevails as the more stable enol tautomer with two mesomeric structures that are separated by only a small barrier (1.7 kcal mol^{-1}).[8] This structure

[a] *University of Bremen, Institute of Applied and Physical Chemistry, Fachbereich 2 (Chemie/Biologie), Leobener Straße/NW 2, Postfach 330440, D-28334 Bremen, Germany. E-mail: j.warneke@uni-bremen.de*
[b] *Zernike Institute for Advanced Materials, University of Groningen, Nijenborgh 4, NL-9747 AG Groningen, The Netherlands*
[c] *Department of Experimental Physics, Comenius University, Mlynska dolina F2, 84248 Bratislava, Slovakia*

† Electronic supplementary information (ESI) available. See DOI: 10.1039/c4cp04239e

This journal is © the Owner Societies 2015

Published on 14 November 2014. Downloaded by University of Groningen on 5/21/2019 9:45:41 AM.

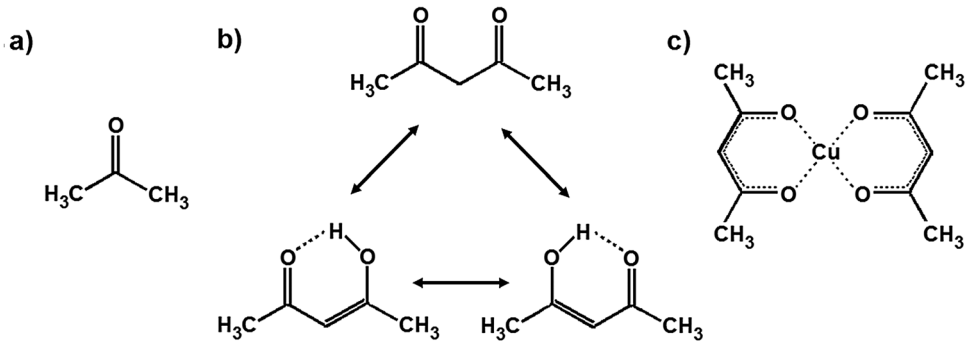

Fig. 1 Molecular structures of (a) acetone, (b) acetylacetone in the keto-form (top) and the enol forms that are preferred in gas and condensed phase[6] (bottom), and (c) copper(II)acetylacetonate as an example of a precursor containing acetylacetonate ligands.

is similar to the delocalized π-system of the ligand in the metal organic precursor complex and thus can serve as model for the latter. Acetone, on the other hand, serves as a reference compound with π-system localized on the carbonyl group.

To obtain a comprehensive view of the electron-induced reactions occurring in condensed layers of acetone and acetylacetone, the products were studied by a combination of methods. First, molecular films were exposed to electrons with kinetic energy (E_0) of 500 eV as usually employed in fundamental studies on FEBID reactions.[4,9,10] Non-volatile reaction products remaining on the surface were investigated by X-ray photoelectron spectroscopy (XPS). To achieve mechanistic insights, we studied the decomposition reactions triggered by irradiation with low energy electrons. This was done by studying the volatile products that undergo electron-stimulated desorption (ESD) during irradiation with low energy electrons and performing post-irradiation thermal desorption spectrometry (TDS) to monitor the volatile products within the molecular layer. Here, an investigation of the dependence on E_0 of the reactions aimed at distinguishing between reactions induced by different electron molecule interactions, namely DEA (dissociative electron attachment) and DI (dissociative ionization). The electron kinetic energies (E_0 between 0 and 40 eV) chosen for these experiments cover the energy range of secondary electrons produced under high-energy electron exposure[2,11] that are known to make a significant contribution to the reactions.[12,13]

These experiments were complemented by comparative gas-phase studies on dissociative electron attachment (DEA) and dissociative electron impact ionization (DI) of the two compounds to investigate the electron-induced fragmentation processes of the isolated molecules. Gas phase experiments on molecular dimers gave insight on the influence of adjacent molecules and therefore allowed us to bridge the gap between the results from gas and condensed phases.

2. Experimental section

2.1. XPS measurements

The X-ray photoelectron spectroscopy experiments were performed in Groningen in ultrahigh vacuum (UHV) at a base pressure of 8×10^{-10} mbar or better, with a Scienta R4000 high energy-resolution spectrometer equipped with a monochromatic Al K_α source ($h\nu$ = 1486.6 eV). The photoelectrons were collected in normal emission. The energy resolution was 0.40 eV. The XPS spectra were analysed using the least-squares curve fitting program Winspec developed at the L.I.S.E. laboratory of the University of Namur, Belgium. Binding energies are reported ±0.05 eV and referenced to the C1s alkyl signal of acetone at 285.0 eV.[14] Deconvolution of the spectra included a Shirley baseline subtraction and fitting with a minimum number of peaks (Voigt profile) consistent with the structure of the molecules on a surface, taking into account the experimental resolution. The uncertainty on the intensity determination was 1% for carbon and 2% for oxygen. Acetone (Sigma-Aldrich, 99.5%) and acetylacetone (ACROS ORGANICS, 99+%) were contained in a stainless steel reservoir at room temperature and introduced into the UHV chamber through a leak valve. The compounds were condensed onto a cooled Ag foil ($T \leq 150$ K) by backfilling the UHV chamber (to 5×10^{-7} mbar for acetone and 5×10^{-8} mbar for acetylacetone). Prior to dosing the precursor onto the Ag foil, the latter was cleaned by Ar^+ sputtering at 1 kV and its cleanliness was verified by XPS.

A Kimball Physics ELG-2 electron source was used for the electron irradiation. The beam was scanned to ensure a uniform illumination. The kinetic energy of the electrons was set to 500 eV. Beam currents were measured with a Faraday cup and the beam current densities were varied between 0.8 and 5.4 μA cm^{-2}. The composition of the gas phase was analysed with a MKS Vac Check mass spectrometer with a maximum detection range of m/z = 100.

2.2. ESD and TDS experiments

All experiments were performed in Bremen using an ultrahigh vacuum (UHV) chamber[15] with a base pressure of about 10^{-10} Torr. For the experiments, thin molecular films were deposited on a polycrystalline Au sheet held at 35–38 K by a closed-cycle helium refrigerator (Leybold Vacuum). To produce these films, vapours of acetone (Sigma-Aldrich, 99.5%) or acetylacetone (ACROS ORGANICS, 99+%) were introduced *via* a gas handling manifold consisting of precision leak valves and a small calibrated volume where the absolute pressure is measured with a capacitance manometer. For each film deposition a calibrated amount of vapour was leaked *via* a stainless steel

Published on 14 November 2014. Downloaded by University of Groningen on 5/21/2019 9:45:41 AM.

capillary opening onto the metal substrate. Prior to each deposition the substrate was cleaned by heating to 400 K using two thin Ta resistive heating ribbons spot-welded to the thicker Au sheet.

The film thickness of acetone was estimated by thermal desorption spectrometry (TDS) of films with increasing coverage (see ESI†). The acetone desorption data for 43 amu show a weak but characteristic peak between 150 and 220 K which rapidly saturates and is therefore ascribed to the monolayer. A second peak with maximum at 140 K starts to increase upon saturation of the monolayer peak and is hence attributed to the successive layers no longer in contact with the substrate. In all experiments, multilayer films with thickness between 6 and 15 layers were prepared. For acetylacetone, the evaluation of the integrated desorption peaks indicated that deposition with reproducible thickness was not achieved. This is due to strong adsorption of the vapour in the inlet system and vacuum chamber and rules out a quantitative comparison of results on acetone and acetylacetone. However, in all experiments on acetylacetone, the well-defined and constant position of the desorption peak maximum at 170 K (see ESI†) supported the assumption of a coverage well in the multilayer regime so that a qualitative comparison between the reactions of the two compounds is valid. For comparison, coverage dependent peak maxima shifting between 170 K and 240 K were obtained for small amounts of vapour as characteristic of the monolayer regime.

Electron-stimulated desorption (ESD) and thermal desorption spectrometry (TDS) were performed by use of a quadrupole mass spectrometer (QMS) residual gas analyser (Stanford, 200 amu) with electron impact ionization at 70 eV. The sample temperature was measured using a type *E* thermocouple press-fitted to the Au substrate. A temperature ramp of 1 K s^{-1} was applied by resistive heating during TDS experiments. Electron exposure was performed with a commercial flood gun (SPECS FG 15/40) delivering electrons with tunable kinetic energy (E_0) at an estimated resolution of the order of 0.5–1 eV and currents of the order of a few μA cm^{-2}, as measured at the substrate.

2.3. Gas phase experiments

The measurements of electron ionization (EI) and electron attachment (EA) processes on gas phase isolated molecules and molecular aggregates were performed in Bratislava using two crossed electron and molecular beam setups operating in high vacuum under single collision conditions.

Isolated molecules were studied in a previously described apparatus[16] that creates a molecular beam by effusion of the vapors from liquid or solid samples *via* a capillary into the reaction region where it is crossed with a perpendicular electron beam.

Electron interactions with molecular aggregates were studied using an apparatus developed and previously used at FU Berlin.[17] Here, the beam containing small molecular aggregates (clusters) is formed in a differentially pumped setup *via* continuous adiabatic expansion of the molecular sample seeded in argon into the vacuum through a 40 μm nozzle held at room temperature. Acetone (Sigma-Aldrich, 99.5%) and acetylacetone (ACROS ORGANICS, 99+%) were mixed with argon at a ratio of 1 : 100 and stagnation pressure before expansion was 3 to 4 bar.

In both experiments, the electron beam was generated by trochoidal electron monochromator operated at an energy resolution around 250 meV FWHM. The electron energy scale for EI studies was calibrated using the threshold of Ar^+ formation at 15.76 eV[18] and for EA and DEA studies by referencing to the SF_6^- formation from SF_6 peaking at ~0 eV.[19] Ions resulting from electron–molecule interactions are extracted by a weak electric field from the reaction region into the quadrupole mass analyzer. The mass separated ions (according to *m*/*z*) are detected using an electron multiplier operating in pulse counting mode. In the experiments, either mass spectra of ions produced at fixed electron energy or ion yield curves for fixed ion mass as a function of the electron energy were recorded. The thresholds of ionization reactions were evaluated by fitting the expected cross section dependence on electron energy $S(\varepsilon)$ to the measured data according to

$$S(\varepsilon) = b;\ \varepsilon < \mathrm{AE}$$

$$S(\varepsilon) = b + a(\varepsilon - \mathrm{AE})^d;\ \varepsilon > \mathrm{AE}$$

were ε represents electron energy and b, a, d are fit parameters. The fitting procedure also takes into account the energy distribution of the electron beam.[16]

2.4. Calculations

The energetics of reactions of selected fragments produced in the condensed molecular layers by electron impact were investigated by use of quantum chemical calculations to support the experimental findings. The calculations were performed at the B3LYP/6-311+G(d,p) level of theory using the Gaussian98 package,[20] using RB3LYP and UB3LYP methods for closed shell and open shell species, respectively. The Berny algorithm was used for geometry optimizations. All minima and transition states were confirmed from analyses of their vibrational frequencies.

3. Results

3.1. XPS of pristine and irradiated layers of acetone and acetylacetone

The C1s core level regions of the XPS spectra of condensed acetone and acetylacetone films prior to and after extended electron exposure are shown in Fig. 2. Two contributions can be identified by comparison with literature,[14,21] one for the oxygen bound carbon and one for alkyl carbons. For acetone, the signal of the methyl groups (285.0 eV) is well separated from the carbonyl signal (287.8 eV) (Fig. 2a) and the latter disappears completely during electron irradiation while a hydrocarbon signal remains even after extensive exposure (Fig. 2b and e). The hydrocarbon signal shifts from 285.0 eV to 284.5 eV (Fig. 2f) in line with the loss of adjacent carbonyl groups. The total carbon intensity loss (from Fig. 2a to b) was determined to be approximately 50%. For acetylacetone (Fig. 2c), the different hydrocarbon C1s signals have very similar chemical shifts and are not resolved (284.9 eV). The chemical shift of the oxygen bound carbons (287.2 eV) is significantly different from the

 This journal is © the Owner Societies 2015

Published on 14 November 2014. Downloaded by University of Groningen on 5/21/2019 9:45:41 AM.

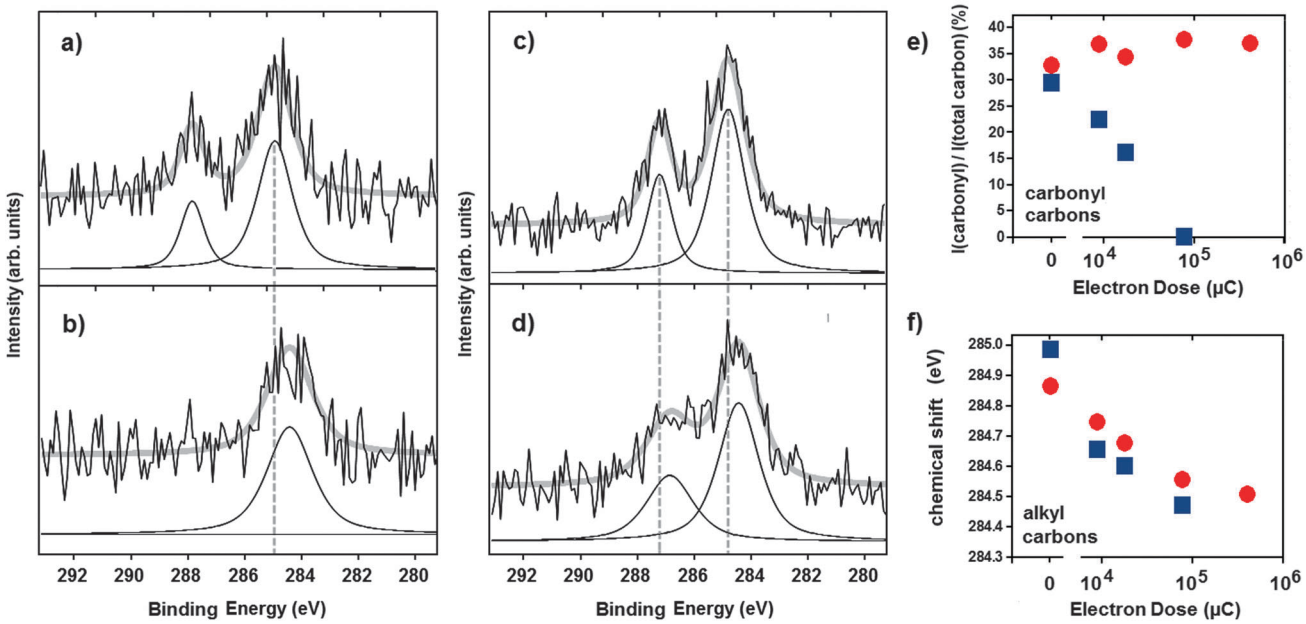

Fig. 2 C1s core level region of the XPS spectra of acetone (a) before and (b) after electron exposure of 0.1 C at E_0 = 500 eV and of acetylacetone (c) before and (d) after electron exposure of 0.4 C at E_0 = 500 eV. The multilayer films were deposited and measured at 110 K. Variation of (e) the C1s intensity due to oxygen bound C species expressed as percentage of the total C1s signal for acetone (blue square) and acetylacetone (red dots) and of (f) the chemical shifts of alkyl carbons with electron exposure for acetone (blue square) and acetylacetone (red dots).

value observed for acetone in agreement with the different carbon–oxygen binding situation of the delocalized π electron system. In contrast to the results for acetone, the relative intensity of the hydrocarbon and carbonyl C1s signals did not change considerably in the case of acetylacetone (Fig. 2d and e), even though a much higher electron exposure was applied. Similar to acetone, the hydrocarbons signal shifts to 284.4 eV after exposure (Fig. 2f). The intensity maximum of the carbonyl C1s peak shifts to 286.7 eV (Fig. 2d) pointing to the formation of ether groups.[14] The total carbon intensity loss (from Fig. 2c to d) was determined to be approximately 10%.

Changes in the O1s spectra (see ESI†) are consistent with the behaviour observed in the C1s spectra. In particular, the intensity decreases strongly in the case of acetone but not for acetylacetone. However, a detailed interpretation of the O1s spectra is not given because of traces of water that could not be eliminated from the surface and thus give rise to a peak overlapping with the signals of acetone, acetylacetone and their irradiation products. Overall and as further pursued in Section 3.2, the data imply that much smaller amounts of volatile products are released from acetylacetone than from acetone.

3.2. Electron-stimulated desorption from condensed layers of acetone and acetylacetone

Mass spectra recorded during electron exposure of condensed multilayer films of acetone and acetylacetone kept at 38 K point to decomposition of the molecules. As shown for bombardment with 30 eV electrons in Fig. 3, irradiation leads in both cases to desorption of CO as well as CH_4 and CH_3. This qualitative picture was observed independent of E_0 between 20 eV and 500 eV. The fragmentation pattern of CH_3 radicals overlaps with that of CH_4.

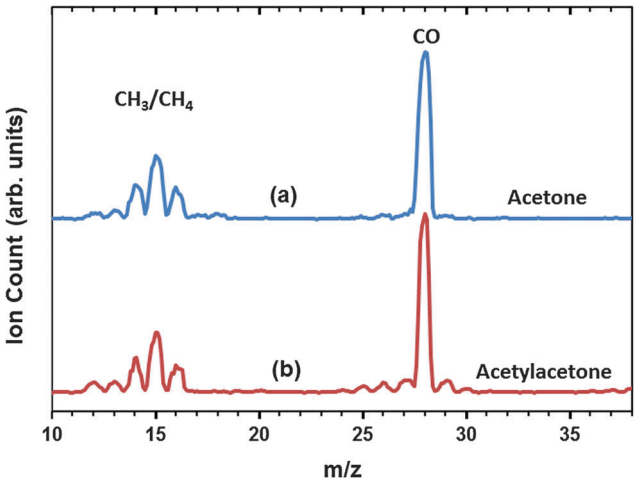

Fig. 3 Mass spectra of products desorbing from condensed multilayer films of (a) acetone and (b) acetylacetone at 38 K immediately after the start of the irradiation with electrons of kinetic energy E_0 = 30 eV.

Nonetheless, in accord with previous studies,[22–24] release of CH_3 is evident from the high intensity of m/z = 15 as compared to m/z = 16. Both signals have roughly comparable intensities in the case of pure CH_4 (see Section 3.3).

Production of CH_4 implies that a new CH bond is formed. The required hydrogen atom can either stem from reactant molecules within the condensed layer or from residual gas in the chamber. To distinguish between these two possibilities, the experiment was repeated using acetone-d_6. Fig. 4 compares the resulting mass spectra within the mass range up to m/z = 20 (CD_4). CD_4 generated in the condensed layer by reaction with adjacent

Published on 14 November 2014. Downloaded by University of Groningen on 5/21/2019 9:45:41 AM.

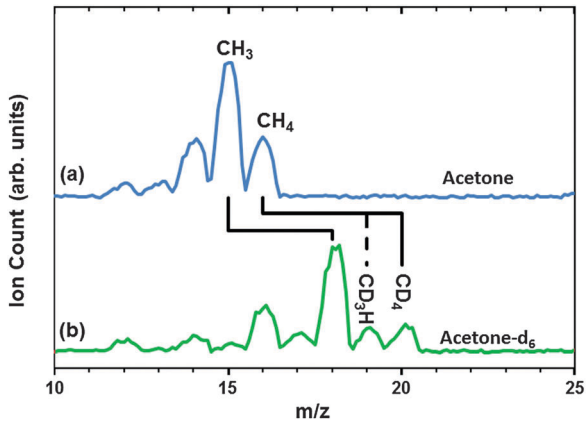

Fig. 4 Mass spectra of products desorbing from condensed multilayer films of (a) acetone and (b) acetone-d_6 at 38 K immediately after the start of the irradiation with electrons of kinetic energy E_0 = 23 eV.

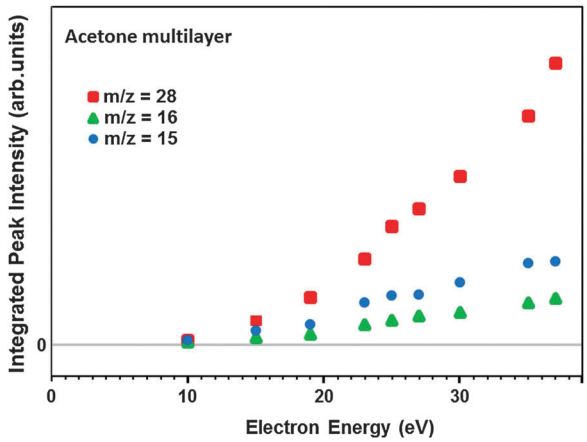

Fig. 5 Yield of fragments desorbing from acetone multilayer films during electron irradiation as a function of the kinetic energy of the electrons. The intensities of the signals detected by mass spectrometry for each kinetic energy were normalized by dividing by the actual current incident on the sample.

acetone-d_6 and desorbed during irradiation is detected as CD_4^+ (m/z = 20). Desorbing CD_3 radicals that react with hydrogen from the residual gases in the vacuum chamber yield CD_3H^+ (m/z = 19). In the case of the acetone-d_6, both m/z = 19 and m/z = 20 are observed. This shows that a part of the methyl radicals released from acetone under electron exposure is indeed converted to methane by reactions with residual hydrogen that presumably occur at surfaces within the chamber.[22]

The relative yields of detected CH_4 and CH_3 can be derived from the ESD data for acetone and acetylacetone (Fig. 3) using the following procedure: first, the mass spectrum of CH_3 was obtained from Fig. 3(a) by subtracting a measured spectrum of CH_4 under the assumption that m/z = 16 stems from only the latter. Using tabulated total ionization cross sections for the two compounds,[25] the relative partial cross sections for formation of CH_3^+ from CH_3 and CH_4^+ from CH_4 can be derived. By normalizing the observed intensity ratio of m/z = 15 from CH_3 and m/z = 16 from CH_4 with the ratio of these partial cross sections, an estimate of the relative amounts of these detected products has been derived and found to be roughly $CH_3 : CH_4$ = 3 : 2. Taking into account the results for acetone-d_6, the ratio of products formed inside the film must be even higher. This leads to the conclusion that during electron irradiation of acetone and acetylacetone films methyl desorption is more pronounced than methane desorption.

To obtain a better insight into the reactions occurring inside the condensed films during irradiation, also the relative amount of desorbing CO needs to be considered. For acetone, characteristic masses of desorbing products (m/z = 28,15,16) as obtained from an average over several scans were observed with intensity ratios of 1 : 0.50 : 0.25. Considering the overlap of the CH_4 and CH_3, the fragmentation patterns and the total ionization cross sections of all three compounds,[25] we can conclude that the amount of desorbing CO is about twice as high as the amounts of CH_3 and CH_4 combined. This ratio does not change noticeably with the electron kinetic energy (E_0) between the ionization threshold and 40 eV as shown in Fig. 5. All intensities increase continuously with increasing E_0 as characteristic of an ionization-driven process.[12] It must be noted that minor amounts of desorbing CO, CH_3, and CH_4 were even observed at E_0 down to about 7 eV. However, these ESD signals were too small for a quantitative analysis and are thus not included in Fig. 5.

Inspection of Fig. 3 suggests that the product ratios observed in ESD from acetylacetone are similar to those estimated above for acetone. However, these ratios may change with increasing irradiation time. Fig. 6 therefore shows the evolution with irradiation time of ESD signals recorded for E_0 = 30 eV. The relative amounts of the products desorbing from condensed acetone films did not change considerably during the first minute of irradiation although the yields decreased by nearly 50%. The CO signal remains higher at longer exposure times when the CH_3 signal already returns to the baseline (Fig. 6(a)). In contrast, the ratio of the amounts of products desorbing from condensed acetylacetone varied with increasing exposure time (Fig. 6(b)). More strikingly, the intensities continued to increase after the initial rise at the start of irradiation and reach a maximum at different times for each individual product, indicating that their release is delayed in the case of acetylacetone. This behaviour is also reflected in the dependence of ESD yields on E_0. If the threshold for product desorption is defined as the E_0 value at which the particular signals increased to an intensity of three times the background noise, this threshold was found to fall between 7 and 12 eV in the case of acetone (compare Fig. 5 and discussion above), while for acetylacetone comparable intensities were obtained only between 15 and 18 eV.

In conclusion, condensed films of both acetone and acetylacetone release CO, CH_4, and CH_3 during electron exposure. However, the present ESD results show that the product desorption kinetics for the two compounds is strikingly different. It must, in addition, be noted that the desorption rate of products measured in ESD experiments on both compounds increased with increasing film thickness. This is in contrast to earlier experiments on photodesorption where signals saturated near monolayer

 This journal is © the Owner Societies 2015

Published on 14 November 2014. Downloaded by University of Groningen on 5/21/2019 9:45:41 AM.

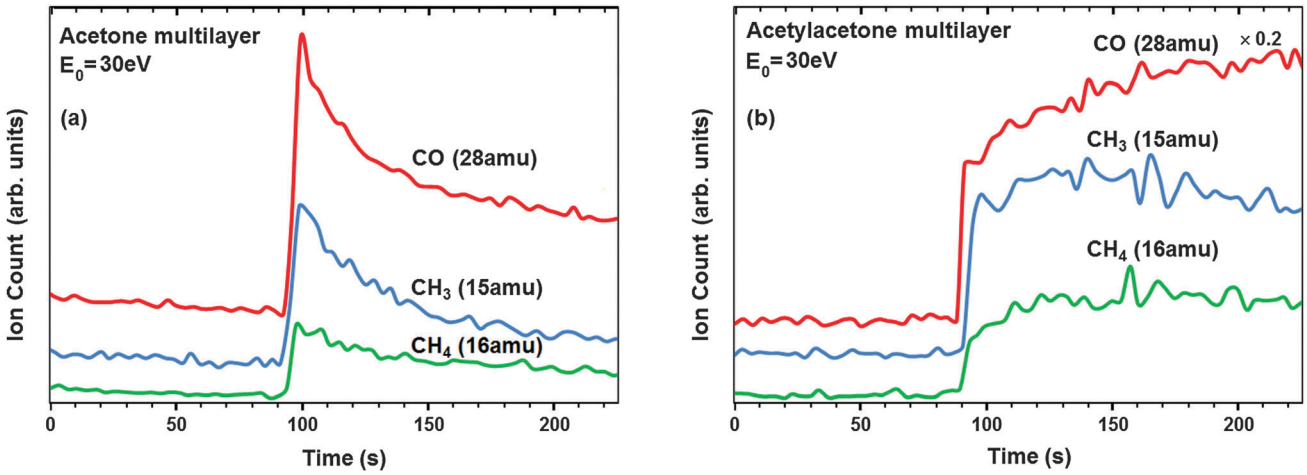

Fig. 6 Evolution with irradiation time of ESD signals recorded for selected masses of fragments desorbing from (a) acetone and (b) acetylacetone multilayers held at 38 K at a kinetic energy of the electrons of 30 eV. Irradiation was started at 90 s. Although a quantitative comparison of intensities is not possible (see Experimental section) it should be noted that total intensities were in general more than an order of magnitude lower in the case of acetylacetone.

coverage indicative of desorption from the topmost layer[26] and points towards a porous nature of the films in accord with the low deposition temperature in the present experiments.[27]

3.3. Post-irradiation thermal desorption spectrometry of condensed layers of acetone and acetylacetone

An estimate of the relative yields of different products must also account for products that remain in the condensed film because the temperature at which the ESD experiment proceeded is too low to induce desorption. Therefore, TDS experiments were performed on the condensed layers following the ESD experiments. As shown in Fig. 7, CO and CH_4 were present in both acetone and acetylacetone films. Here the intensity ratio of the signals m/z = 16 and m/z = 15 is the one characteristic for CH_4,[28] suggesting that any CH_3 that has not desorbed during irradiation rapidly reacts within the film to yield other products.

The procedure described in Section 3.1 was also used to derive from the TDS data information on the relative amounts of CO as compared to the sum of CH_4 and C_2H_6 remaining in the condensed layer following electron exposure. Similar to the ESD data, CO is more abundant than the combined amounts of CH_4 and C_2H_6 in both acetone with ratio 2 : 1 and in acetylacetone (5 : 1), independent of electron energy, electron dose or film thickness. For both compounds, the amount of hydrocarbon material recovered as volatile species by TDS and ESD is thus considerably smaller than anticipated from the relative amounts of carbonyl and hydrocarbon groups in acetone and acetylacetone. This points towards the formation of additional products that are not seen in these experiments, in good agreement with XPS results shown in Section 3.1.

A striking difference between acetone and acetylacetone is that the formation of ethane is observed in the case of former but not for the latter (Fig. 7). This difference might be explained

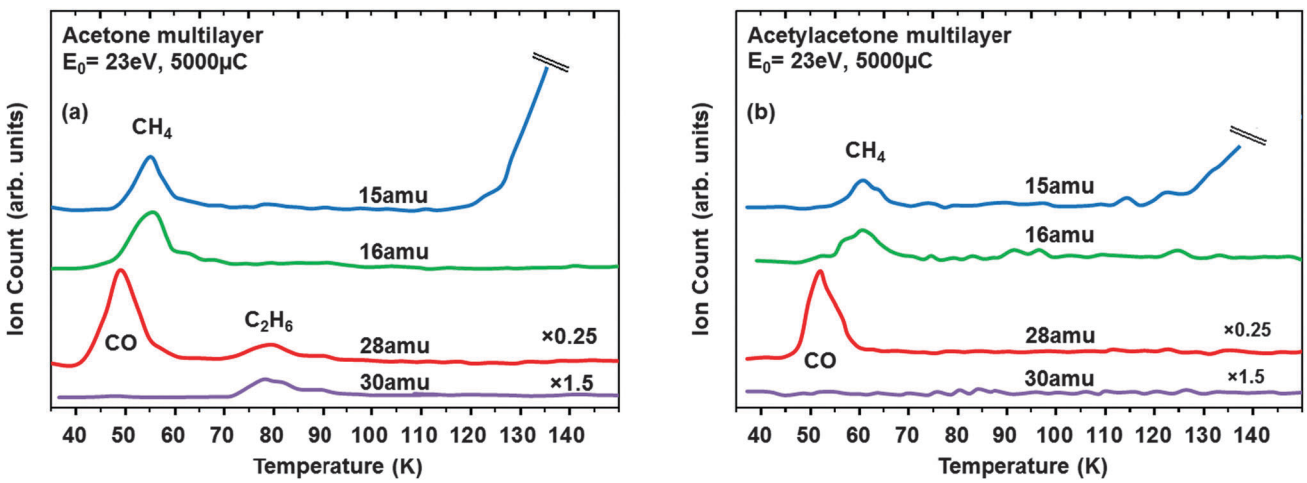

Fig. 7 Thermal desorption from (a) acetone and (b) acetylacetone multilayers recorded for selected masses following an electron exposure of 5000 μC at E_0 = 23 eV and 38 K.

Published on 14 November 2014. Downloaded by University of Groningen on 5/21/2019 9:45:41 AM.

by an intramolecular reaction whereby the two methyl groups of the reactant yield ethane. Such a reaction is not expected to be favourable in the case of acetylacetone because it implies the expulsion of a reactive species while acetone would release stable CO instead. To investigate if an intermolecular formation of ethane is in fact preferred, the experiment was repeated on a sample containing equal amounts of acetone and acetone-d_6. While C_2H_6 desorbed abundantly, C_2D_6, identified by m/z = 36, was detected in only very small amounts near the detection limit. This effect can be attributed to the lower mobility of the heavier CD_3 compared to CH_3 or to a smaller electron impact ionization cross section of acetone-d_6. However, the experiment revealed besides these expected products the formation of CH_3CD_3 as evident from TDS signals for m/z = 33 and m/z = 31. These results strongly indicate that a statistical recombination of mobile methyl radicals occurs. The lack of ethane formation in acetylacetone thus suggests, in accord with the smaller ESD yield of CH_3, that also the concentration of CH_3 radicals in the acetylacetone films remains low during electron irradiation for reasons discussed in the following sections.

3.4. Dissociative ionization and electron attachment to acetone and acetylacetone in the gas phase

The results of the condensed phase experiments described so far show that the desorption of small fragments such as CH_3 and CO proceeds much more easily, *i.e.* with higher yield and at lower E_0, from condensed layers of acetone than from acetylacetone. Therefore, we revisited the electron-induced dissociative ionization (DI) and the dissociative electron attachment (DEA) of single acetone and acetylacetone molecules in the gas phase to reveal if the formation of such small fragments occurs for electrons with different E_0 in the two compounds and can thus explain the differences observed in the condensed layers.

DEA to acetone[29,30] has been investigated before but only one study exists for acetylacetone.[31] The highest DEA yields have been obtained for electrons with kinetic energy E_0 close to the threshold for desorption, the latter seen in Fig. 5. Therefore a direct comparison of DEA to acetone and acetylacetone was performed here to reveal potential differences and verify if the latter can explain the more facile electron-induced decomposition of acetone films as well as the easier desorption of CH_3 and CO from these solid films under electron irradiation.

The mass spectra in the top panel of Fig. 8 clearly show that DEA of acetone and acetylacetone in the gas phase proceeds in a similar fashion. This becomes even more evident if one compares the energy dependence of anion yields for both compounds, shown in the bottom panel of Fig. 8, which are very similar to the previous findings[29–31] although the maxima are shifted by about 1 eV to higher energy. DEA takes place at very similar E_0 for all fragments, except for formation of $[M–H]^-$ which occurs at much lower E_0 in the case of acetylacetone (m/z = 99) as compared to acetone (m/z = 57), most likely because the delocalized π-electron system of the remaining fragment has a larger electron affinity than the corresponding fragment of acetone. Also note that $[M–H_3CCO]^-$ in acetylacetone (m/z = 57) and CH_3^- (m/z = 15) in both compounds result from the same

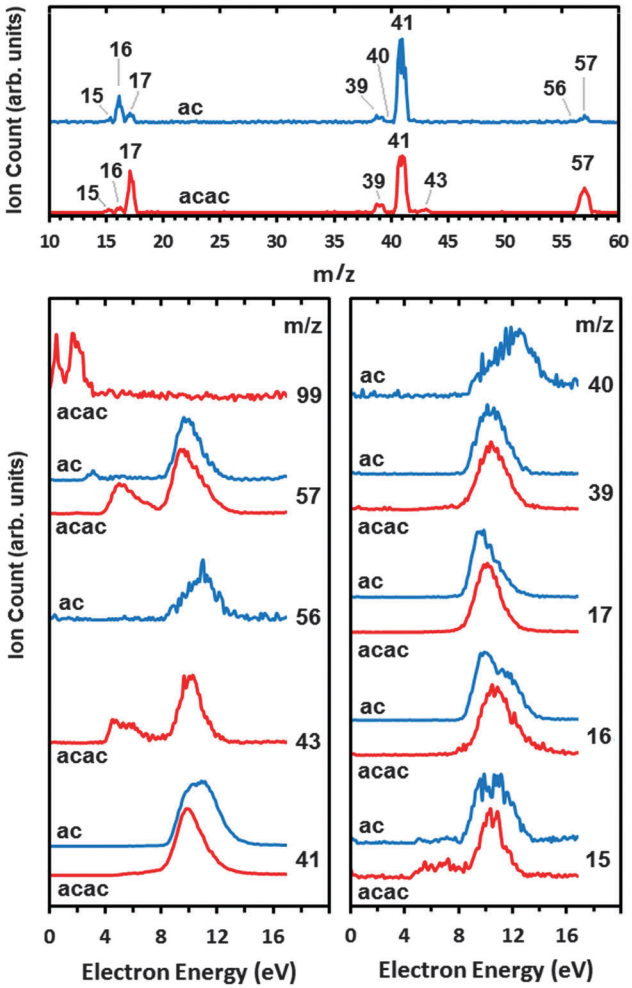

Fig. 8 Top panel: negative ion mass spectra of acetone (blue, ac) and acetylacetone (red, acac) obtained in the gas phase by crossing a molecular beam of each compound with electrons of kinetic energy E_0 = 9.5 eV (maximum of the total ion current). Bottom panels: ion yield curves of all detected anion fragments as a function of the kinetic energy of the impinging electrons. Note that all curves were arbitrarily scaled to the same height but offset for clarity. Their true relative intensities can be estimated from the mass spectra.

type of bond cleavage which is again reflected in very similar resonance positions. The ion yield curves for m/z = 41 ($HCCO^-$),[29] m/z = 39 ($C_3H_3^-$),[30] m/z = 17 (OH^-)[29] and m/z = 16 (O^-)[29] match closely, pointing again to analogous DEA processes for acetone and acetylacetone.

Regarding the typical threshold behaviour seen in the dependence of ESD on the kinetic energy of the electrons (Fig. 5), DI is the most likely mechanism to drive the decomposition of condensed layers of acetone and acetylacetone. It must be noted here that gas phase thresholds for DI are expected to differ from ESD thresholds because charged fragments in the latter situation must overcome the barrier resulting from polarization forces in the surrounding medium. However, as is most important here, the thresholds for fragmentation do not differ largely between acetone and acetylacetone, as seen from the comparison of the values reported in Table 1. In particular, α-cleavage yielding $[M–CH_3]^+$

 This journal is © the Owner Societies 2015

Published on 14 November 2014. Downloaded by University of Groningen on 5/21/2019 9:45:41 AM.

and the corresponding CH_3 radical sets in at very similar E_0 in both compounds and thus does not rationalize their different behaviour in ESD. Here it must be noted that for acetylacetone the abstraction of a CH_3 radical dominates at low E_0 although m/z = 43 (H_3CCO^+) becomes the dominant ion fragment at 70 eV.[28] The yield of CH_3^+ on the other hand remains lower than that of H_3CCO^+ at all investigated E_0.

These results clearly show that DEA or DI processes of the isolated molecules cannot explain the differences in electron-induced reactivity observed in condensed films of acetone and acetylacetone. Intermolecular interactions must thus be responsible for the differences described in 3.1 to 3.3.

3.5. Gas phase cluster experiments

To bridge the gap between condensed and gas phase experiments, we also performed DI measurements of acetone and acetylacetone clusters. The molecular beams containing both isolated molecules and clusters were crossed with a 70 eV electron beam and mass spectra were collected. The results are shown in Fig. 9. In this experiment m/z values ranging from 50 to 450 were scanned revealing the formation of clusters consisting of two and three acetone molecules. Please note that signals of isolated acetone molecules and the corresponding fragments occur in the low mass range and therefore overlap with the very large signal of Ar, which was used as carrier gas for the supersonic expansion in these cluster experiments. However, the fragmentation behaviour of isolated acetone molecules is well known and described also in Section 3.4.

In the case of acetylacetone, the monomer and the dimer were detected. The expected loss of CH_3 was observed for both the acetone clusters (Fig. 9(a) and (b)) and for the isolated molecule (Table 1). However, while the acetylacetone monomer also shows the expected $[M–CH_3]^+$ signal (Fig. 9(c) and Table 1), the loss of CH_3 was not detected for the acetylacetone dimer (Fig. 9(d)). Apparently, CH_3 radicals are retained within acetylacetone aggregates. This finding rationalizes the lower yield of CH_3 in ESD from condensed layers of this compound.

4. Discussion

The combined results of XPS, ESD and TDS experiments on electron-induced reactions in multilayer films of acetone and acetylacetone reveal striking differences. XPS shows that a much higher amount of non-volatile material remains at the surface in the case of electron irradiation of acetylacetone. Also oxygen is incorporated in this deposit while acetone predominantly yields

Table 1 Measured fragmentation thresholds for DI fragments of acetone and acetylacetone

Acetone	Threshold (eV)		Acetylacetone	Threshold (eV)	
Fragment	This work	Literature[18]	Fragment	This work	Literature[18]
$[CH_3COCH_3]^{+\bullet}$	9.85–9.91	9.71–9.74	$[CH_3COCHCOHCH_3]^{+\bullet}$	9.24–9.32	8.85–9.63
$[CH_3CO]^+$	10.53–10.58	10.28–11.30	$[COCHCOHCH_3]^+$	10.29–10.36	10.7
			$[CH_3CO]^+$	10.57–10.63	—
$[CH_3]^+$	14.74–14.91	14.93–15.36	$[CH_3]^+$	14.39–14.32	—

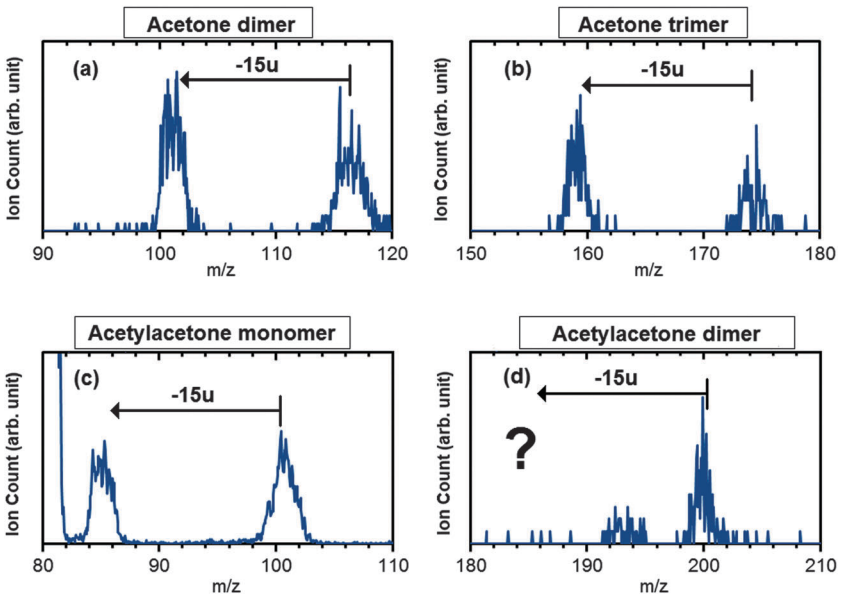

Fig. 9 Positive ion mass scans collected when crossing the supersonic molecular beams of acetone and acetylacetone with a beam of electrons with a kinetic energy of 70 eV. The data show loss of CH_3 from (a) an acetone dimer, (b) an acetone trimer and (c) an acetylacetone monomer. Note that the intense signal at m/z = 80 relates to Ar_2^+. In the case of the acetylacetone dimer (d) no loss of CH_3 was observed.

Published on 14 November 2014. Downloaded by University of Groningen on 5/21/2019 9:45:41 AM.

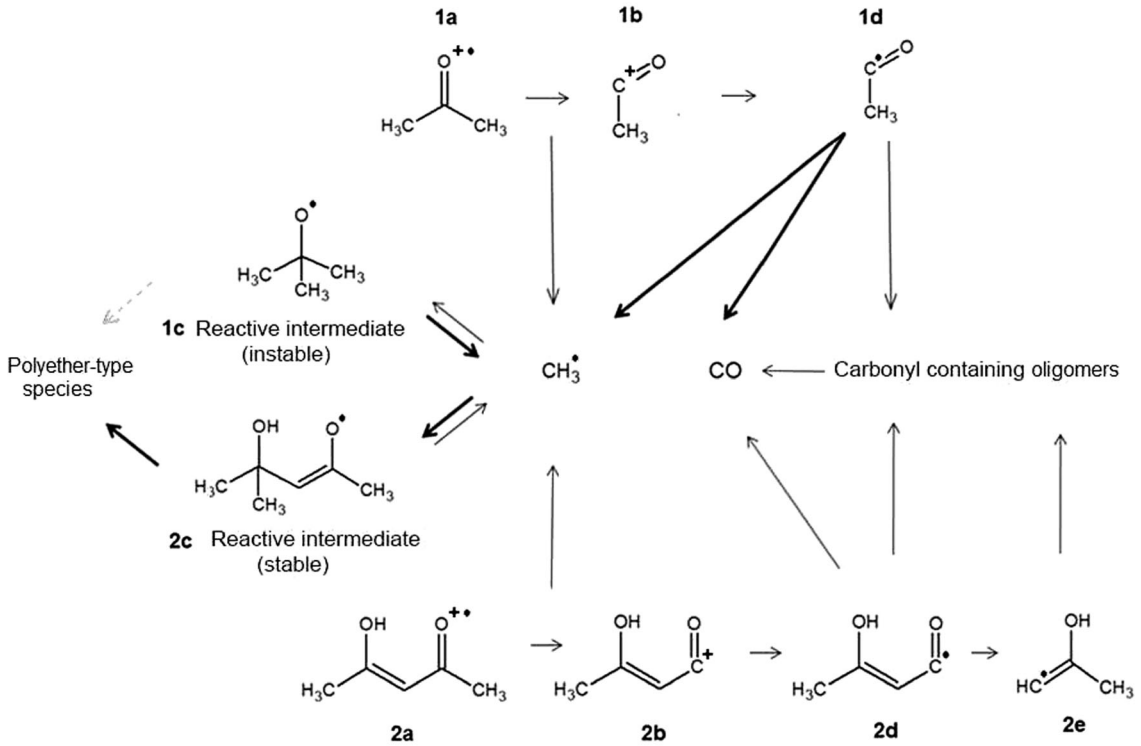

Fig. 10 Proposed reaction scheme for the electron-induced decomposition of condensed layers of acetone and acetylacetone summarizing the mechanisms discussed in the text. The formation of larger species implies reaction with intact acetone and acetylacetone, respectively.

a hydrocarbon residue after extensive electron exposure. In ESD from acetylacetone, lower desorption rates of the volatile products CO, CH_3, and CH_4 were observed than in the case of acetone. While the desorption rate from acetone decreases continuously with increasing electron exposure, it increases during the first stages of exposure of acetylacetone before finally dropping. TDS reveals that C_2H_6 is produced during electron irradiation in acetone layers but not in acetylacetone. As a related finding, gas phase experiments show that expulsion of CH_3 following electron-induced ionization occurs in the acetylacetone monomer but is suppressed in the dimer. The following discussion is supported by a reaction scheme in Fig. 10 with molecular structures labelled by bold numbers in the text.

4.1. Initial fragmentation reaction: methyl formation

Among the volatile products detected in ESD, only CH_3 can result from dissociation of a specific bond without further reaction or rearrangement. We consider here the different electron-induced fragmentation processes yielding CH_3.

4.1.1. Dissociative electron attachment (DEA). Considering first the anionic route to dissociation, the dominant DEA channel for acetone, *i.e.* the formation of $HCCO^-$ (m/z = 41) observed when the electron kinetic energy reaches around 10 eV, may be accompanied by release of CH_3 according to ref. 29 as described by eqn (1).

$$(H_3C)_2CO + e^- \rightarrow [(H_3C)_2CO]^{\bullet -} \rightarrow HCCO^- + CH_3^{\bullet} + H_2. \quad (1)$$

If we assume a similar bond cleavage and rearrangement in acetylacetone, an acetonyl radical in its enol form would be released instead of CH_3 according to eqn (2)

$$H_3CC(O)CH{=}C(OH)CH_3 + e^- \rightarrow [H_3CC(O)CH{=}C(OH)CH_3]^{\bullet -} \rightarrow HCCO^- + CH{=}C(OH)CH_3^{\bullet} + H_2 \quad (2)$$

Thus, DEA as the dominant reaction channel explains the higher production of methyl from acetone as compared to acetylacetone. However, our ESD experiments do not show a peak in CH_3 intensity at or near the gas-phase DEA process (E_0 = 10 eV). In fact, the continuous increase with electron kinetic energy of the desorption rates in ESD (Fig. 5) suggests that electron impact ionization predominantly drives the reaction that leads to volatile products. We therefore conclude that dissociation through DEA plays only a minor role in the formation of volatiles.

4.1.2. Dissociative ionization (DI). In both acetone (**1a**) and acetylacetone (**2a**) the release of CH_3 also proceeds *via* a cationic route as described by eqn (3) and (4). It is triggered by direct ionization followed by α-cleavage, yielding $[M–CH_3]^+$ (**1b**,**2b**).

$$(H_3C)_2CO + e^- \rightarrow [(H_3C)_2CO]^{\bullet +} + 2e^- \rightarrow [H_3CCO]^+ + CH_3^{\bullet} + 2e^- \quad (3)$$

$$H_3CC(O)CH{=}C(OH)CH_3 + e^- \rightarrow [H_3CC(O)CH{=}C(OH)CH_3]^{\bullet +} + 2e^- \rightarrow [C(O)CH{=}C(OH)CH_3]^+ + CH_3^{\bullet} + 2e^- \quad (4)$$

 This journal is © the Owner Societies 2015

Published on 14 November 2014. Downloaded by University of Groningen on 5/21/2019 9:45:41 AM.

This is the most efficient ionization-driven fragmentation process near the ionization threshold. However, the reaction is very similar for both compounds as is seen in gas phase experiments on isolated molecules. For an explanation of the differences observed in molecular films, effects of the surrounding material must be considered. Gas phase cluster experiments showed that the presence of a second molecule of acetylacetone, a situation that is also encountered in the condensed phase, suppresses CH_3 release (Fig. 9). We suggest that the released CH_3 radicals are captured by an intact neighbouring molecule. In the case of acetone, addition of CH_3 to the carbonyl carbon atom yields a *tert*-butoxy radical $(CH_3)_3CO$ (**1c**). This oxygen-centred radical is also known to be the reactive intermediate in polymerization reactions initiated by di-*tert*-butylperoxide.[32] However, it is known that *tert*-butoxy radicals are highly instable and also lose CH_3 as concurrent reaction,[32,33] making it unlikely that CH_3 radicals can be retained by addition to acetone.

To understand the stability of these reaction products, theoretical insight is needed (see overview in ESI†). We performed B3LYP/6-311+G(d,p) calculations and found that the *tert*-butoxy radical is placed only 0.14 eV below the isolated reactants CH_3 and acetone. In contrast, the addition of CH_3 to the oxygen-carrying enol carbon of acetylacetone produces a radical (**2c**, Fig. 10) that is stabilized by 0.53 eV with respect to the reactants. Based on the Bell–Evans–Polanyi principle[34] and taking into account that the same type of reactions proceed in both compounds, we conclude that any transition state energy for methyl trapping must be considerably lower in acetylacetone as compared to acetone. Trapping of CH_3 by acetylacetone should thus be faster than trapping by acetone. Considering the calculated energies, also the reverse reaction of this species to release CH_3 is less probable than in the case of the *tert*-butoxy radical. Loss of CH_3 from the carbonyl site is even more unfavourable since an energy of 1.64 eV is required to reach the product. In consequence, CH_3 may be efficiently trapped by acetylacetone, but not by acetone. The observed difference in CH_3 generation from condensed films is thus not related to a different mechanism of formation in the DI process, but rather results from a difference in subsequent capture reactions.

4.1.3. Neutral dissociation (ND). Electron impact can also induce neutral dissociation (ND) *via* electronic excitation of the molecules[12] as described by eqn (5) and (6).

$$(CH_3)_2CO + e^- \rightarrow (CH_3)_2CO^* + e^- \rightarrow (H_3C)CO^\bullet + CH_3^\bullet + e^- \quad (5)$$

$$H_3CC(O)CH{=}C(OH)CH_3 + e^- \rightarrow [H_3CC(O)CH{=}C(OH)CH_3]^* + e^- \rightarrow [C(O)CH{=}C(OH)CH_3]^\bullet + CH_3^\bullet + e^- \quad (6)$$

This may also contribute to the observed products. In fact, both acetone and acetylacetone can be dissociated by photoexcitation at 248 nm, corresponding to an energy of approximately 5 eV.[35] However, as we cannot simultaneously monitor neutral and charged fragments in the present experiments, the contribution of such a process cannot be ascertained.

4.2. Consequences of methyl trapping

The product **2c**, formed by addition of methyl to acetylacetone, is expected to attack, due to its high reactivity, adjacent molecules and eventually form larger and thus less volatile products. Such reactions account for the build-up of non-volatile residues that explain the XPS results of acetylacetone. In contrast, the facile decomposition and the inefficient trapping of CH_3 radicals by acetone is reflected in ESD data. As shown above, for acetone, the CH_3 desorption rate roughly follows an exponential decay and drops to zero after a sufficiently long irradiation time. In contrast, the more efficient trapping of CH_3 by acetylacetone accounts for both the much lower ESD intensities as compared to acetone, and the slow increase of CH_3 desorption during the first stages of electron exposure. As the film is gradually depleted of intact acetylacetone and larger structurally different molecules are formed as discussed above, the CH_3 trapping efficiency decreases. The CH_3 ESD signal increases until the depletion of acetylacetone (as the initial source of CH_3) overcompensates the loss of trapping efficiency.

4.3. Further fragmentation and subsequent reactions

4.3.1. Direct loss of CO. The described hypothesis explains the release (or lack thereof) of CH_3 but the release of CO suggests that further fragmentation of $[M–CH_3]^+$ (**1b**,**2b**) occurs as well. In fact, unlike CH_3, CO cannot be produced by simple bond cleavage but requires more extensive fragmentation. The sudden increase of ESD of CO at the start of irradiation thus indicates that such further fragmentation is a rapid process. On the other hand, based on the energy differences calculated at the B3LYP/6-311+G(d,p) level between products and reactants which represent lower limits to the actual activation energies for the processes, the loss of CO from $[M–CH_3]^+$ requires an excess energy of at least 3.5 eV in the case of $[H_3CCO]^+$ (**1b**), close to a previously reported value,[7] and 3.8 eV for $[HO(H_3C)C{=}CHCO]^+$ (**2b**). However, the onset of ESD of CO already appears between 7 eV and 10 eV in the present experiments and thus even below the gas phase ionization threshold of 9.7 eV.[18] Even when taking into account a stabilization of the positive ion by 1–2 eV in the condensed phase,[7] the dissociation of $[H_3CCO]^+$ (**1b**) would not be expected below roughly E_0 = 10 eV. This suggests that more favourable reaction channels are accessible. The same fragmentation releasing CO is much more facile in the neutral species $[H_3CCO]$ (**1d**) and $[HO(H_3C)C{=}CHCO]$ (**2d**). At the typical current densities applied in the ESD experiments of 20 μA cm^{-2}, each molecule on average encounters an electron about every second. Taking into account Coulomb attraction between a cationic fragment and a thermalized electron in the film, neutralization is quite likely. We therefore expect that the cationic fragmentation pathway transitions into the neutral one. Following neutralization, the fragmentation products CH_3 and CO have an energy of only 0.75 eV above the reactant H_3CCO (**1d**) according to B3LYP/6-311+G(d,p) calculations, again very close to a previously reported value.[7,35] Loss of CO from $[M–CH_3]$ should thus occur at much lower excess energy than from the corresponding cation. Therefore we assume that CO is predominantly released from the neutral fragments.

Published on 14 November 2014. Downloaded by University of Groningen on 5/21/2019 9:45:41 AM.

This reaction is another source of CH_3 radicals in the case of acetone. The analogous reaction in the case of the HO(H_3C)C═CHCO (**2d**) fragment resulting from acetylacetone and yielding HO(H_3C)C═CH (**2e**) and CO requires an energy of at least 1.63 eV as predicted by B3LYP/6-311+G(d,p) only considering the localized structure shown. It is also possible that intermolecular hydrogen transfer delocalizes and stabilizes the radical. The emission of CO is hence less probable in this acetylacetone fragment, explaining the low CO intensity at the start of electron irradiation. Moreover, the reaction of **2d** does not yield CH_3 but the larger and thus less volatile radical fragment **2e**. In consequence, formation of CH_3 in the subsequent fragmentation steps is more likely for acetone. This contributes to the more prominent desorption of CH_3 from acetone layers and also the formation of C_2H_6 by recombination of CH_3 as seen in TDS experiments.

4.3.2. Delayed loss of CO and incorporation in acetylacetone irradiation products. During electron-induced decomposition of acetone, CO desorption rates at first follow the decay of the CH_3 signal but then stay at a non-zero level even for exposures where CH_3 desorption has already levelled off. This points towards the formation of larger carbonyl containing molecules. Such a reaction has been observed before in condensed layers of acetaldehyde.[36] In an analogous reaction, CH_3 radicals released by α-cleavage abstract a hydrogen atom from an intact acetone molecule to form CH_4. The resulting acetonyl radical may recombine with further CH_3 to yield methyl-ethyl-ketone or, in later stages of the reaction, even larger carbonyl containing products. It can also not be excluded that radical fragments like **1d** react with neighbouring molecules before they can decay. This leads to the formation of similar larger structures. Electron-induced α-cleavage of these compounds then leads to release of a larger hydrocarbon radical and, in a subsequent reaction as described above, to CO but not to formation of any more methyl radicals. Such reaction sequences, while initially retaining oxygen, can thus contribute to the production of larger and increasingly less volatile hydrocarbons by recombination of the released alkyl radicals and also explain the delayed desorption of CO. Nonetheless, as the oxygen remains present as carbonyl group in the products of increasing size, it is eventually expulsed from these molecules as CO so that a pure hydrocarbon residue is formed in the end, as evident in XPS.

The radical fragments that are formed by decomposition of acetylacetone (for example **2e**) can react with other molecules within the film to yield structures in which the CO-containing structural element is no longer stabilized by a delocalized π-electron system and can therefore more easily emit CO under electron irradiation. This mechanism explains the increase in CO intensity during ESD. However, the formation of such larger carbonyl-containing molecules, although explaining the acetone results completely, can only play a minor role for acetylacetone because in this case most oxygen remains inside the deposit left on the surface after electron irradiation, as seen in XPS. Therefore the chemical nature of the large molecules formed in irradiated acetylacetone films must be different. Here, the radical resulting from addition of CH_3 to acetylacetone (**2c**) may again play a key role. Instead of undergoing the reverse reaction as in acetone, this oxygen-centred radical can react with an adjacent acetylacetone molecule in analogy to a radical polymerization reaction, namely by attacking one of the oxygen-carrying carbons and thus leading to a polyether-type material. We are not aware of other molecular structures containing C–O bonds that do not emit CO under electron irradiation. For example, CO formation has also been described in the case of alcohols.[37] Under electron impact ionization, however, as known from mass spectrometry, ether compounds do not have a tendency towards release of CO.[38] The same has also been observed in the case of DEA to ethers.[39] This can also be rationalized by the corresponding structure of such a polyether. Neither C–O bond cleavage nor α-cleavage can lead to a fragment that can easily release CO from R_3C–O–CR_3 structures. Breaking of three carbon–carbon bonds and one carbon–oxygen bond would be necessary here. In consequence, oxygen remains incorporated in the residual material after prolonged exposure to acetylacetone.

5. Conclusions

Often, the bad performance of metal acetylacetonates in FEBID has been attributed to the strong binding of the metal to the chelating ligand.[2,4] Our experiments have shown that acetylacetone alone also yields large amounts of residual carbon and oxygen under electron irradiation while small carbonyl containing molecules like acetone decompose much more easily. A first guess for a reasonable explanation could be the larger π-system that stabilizes the acetylacetone molecule. However, gas phase experiments have shown that the energy-dependence of electron induced fragmentation through DI and DEA of single molecules is very similar for acetylacetone and acetone and the stability of the molecule itself is not a reasonable explanation.

We presented here a reaction mechanism (Fig. 10) that is in agreement with all experimental results: the key argument is the trapping of methyl radicals (released by α-cleavage) by neighbouring acetylacetone molecules. The release of CH_3 is energetically less favourable from **2c** than from **1c**. Therefore, desorption of CH_3 from condensed acetylacetone is less likely than from acetone. Instead, acetylacetone forms large and non-volatile products in higher yields than acetone. These reaction products have a chemical structure that does not enable subsequent efficient decomposition. These residues that possibly contain a complex mixture of different products were detected at the surface by post irradiation XPS analysis.

The electronic structure in the ligand of metal-acetylacetonates is similar to that of acetylacetone itself as well as an acetylacetonate anion as both can be described by the two mesomeric structures shown in Fig. 1. Intact acetylacetone is a DI fragment of metal-acetylacetonates[31] while DEA of metal-acetylacetonates produces the free ligand acetylacetonate.[40,41] The described phenomena are therefore expected to contribute considerably to the electron-induced chemistry in FEBID processes. Acetylacetone thus appears to be fundamentally inappropriate as ligand for metals that should be deposited by FEBID in pure form. However, it should be kept in mind, although it is often thought that the decomposition behaviour of precursors is dominated by the ligand architecture

 This journal is © the Owner Societies 2015

Published on 14 November 2014. Downloaded by University of Groningen on 5/21/2019 9:45:41 AM.

that the reaction behaviour might change to some extent in the metal complexes.

Concerning the investigation of fundamental reaction mechanisms in FEBID in general, the present study shows that mass spectrometric investigations on DEA and DI can give valuable insights into the initial electron molecule interaction. However, caution must be exercised when drawing conclusions about processes occurring in the condensed phase. The results presented here show that the reaction mechanisms underlying FEBID can only be understood if reactions of produced fragments inside the condensed film are fully considered.

Acknowledgements

The authors are grateful to Dr Jan Hendrik Bredehöft for very helpful discussions. This work was conducted within the framework of the COST Action CM1301 (CELINA) and the COST Action MP1002 (Nano-IBCT). JW and PS thank the DFG for financial support. WD and PR gratefully acknowledge NanoNed and the Zernike Institute for Advanced Materials. MS, PP and SM would like to acknowledge to Slovak Research and Development Agency for the contract No. APVV-0733-11 and the Slovak Grant Agency VEGA V/0514/12.

References

1 H. O. Pierson, *Handbook of Chemical Vapor Deposition: Principles, Technology, and Applications*, Noyes, Park Ridge, USA, 1999.
2 I. Utke, P. Hoffmann and J. Melngailis, *J. Vac. Sci. Technol., B: Microelectron. Nanometer Struct.*, 2008, **26**, 1197–1276.
3 T. Lukasczyk, M. Schirmer, H. P. Steinrück and H. Marbach, *Small*, 2008, **4**, 841–846.
4 J. D. Wunk, S. G. Rosenberg, J. M. Gorham, W. F. van Dorp, C. W. Hagen and D. H. Fairbrother, *Surf. Sci.*, 2011, **605**, 257–266.
5 A. Luisier, I. Utke, T. Bret, F. Cicoira, R. Hauert, S.-W. Rhee, P. Doppelt and P. Hoffmann, *J. Electrochem. Soc.*, 2004, **151**(8), 535–537.
6 E. Burean and P. Swiderek, *Surf. Sci.*, 2008, **602**, 3194–3198.
7 M. Lepage, M. Michaud and L. Sanche, *J. Chem. Phys.*, 2000, **113**, 3602–3608.
8 X.-B. Chen, W.-H. Fang and D. L. Phillips, *J. Phys. Chem. A*, 2006, **110**, 4434–4441.
9 K. Landheer, S. G. Rosenberg, L. Bernau, P. Swiderek, I. Utke, K. Hagen and D. H. Fairbrother, *J. Phys. Chem. C*, 2011, **115**, 17452–17463.
10 S. G. Rosenberg, K. Landheer, C. W. Hagen and H. D. Fairbrother, *J. Vac. Sci. Technol., B: Nanotechnol. Microelectron.: Mater., Process., Meas., Phenom.*, 2012, **30**, 051805.
11 S. J. Randolph, J. D. Fowlkes and P. D. Rack, *J. Appl. Phys.*, 2005, **97**, 124312.
12 E. Böhler, J. Warneke and P. Swiderek, *Chem. Soc. Rev.*, 2013, **42**, 9219–9231.
13 C. R. Arumainayagam, H.-L. Lee, R. B. Nelson, D. R. Haines and R. P. Gunawardane, *Surf. Sci. Rep.*, 2010, **65**, 1–44.
14 D. T. Clark and H. R. Thomas, *J. Polym. Sci., Polym. Chem. Ed.*, 1978, **16**, 791–820.
15 I. Ipolyi, W. Michaelis and P. Swiderek, *Phys. Chem. Chem. Phys.*, 2007, **9**, 180–191.
16 M. Stano, Š. Matejčík, J. D. Skalny and T. D. Märk, *J. Phys. B: At., Mol. Opt. Phys.*, 2003, **36**, 261–271.
17 O. Ingólfsson, F. Weik and E. Illenberger, *Int. J. Mass Spectrom. Ion Processes*, 1996, **155**, 1–68.
18 S. G. Lias, *et al.*, *Ion Energetic Data, in: NIST Chemistry WebBook, NIST Standard Reference Database Number 69*, 2014http://webbook.nist.gov/chemistry/.
19 L. Christophorou and L. G. Olthoff, *J. Phys. Chem. Ref. Data*, 2000, **29**, 267–330.
20 M. J. Frisch, G. W. Trucks, H. B. Schlegel, G. E. Scuseria, M. A. Robb, J. R. Cheeseman, V. G. Zakrzewski, J. A. Montgomery, Jr., R. E. Stratmann, J. C. Burant, S. Dapprich, J. M. Millam, A. D. Daniels, K. N. Kudin, M. C. Strain, O. Farkas, J. Tomasi, V. Barone, M. Cossi, R. Cammi, B. Mennucci, C. Pomelli, C. Adamo, S. Clifford, J. Ochterski, G. A. Petersson, P. Y. Ayala, Q. Cui, K. Morokuma, D. K. Malick, A. D. Rabuck, K. Raghavachari, J. B. Foresman, J. Cioslowski, J. V. Ortiz, B. B. Stefanov, G. Liu, A. Liashenko, P. Piskorz, I. Komaromi, R. Gomperts, R. L. Martin, D. J. Fox, T. Keith, M. A. Al-Laham, C. Y. Peng, A. Nanayakkara, C. Gonzalez, M. Challacombe, P. M. W. Gill, B. Johnson, W. Chen, M. W. Wong, J. L. Andres, C. Gonzalez, M. Head-Gordon, E. S. Replogleand J. A. Pople, *Gaussian 98, Revision A.6*, Gaussian, Inc., Pittsburgh PA, 1998.
21 J. L. Armstrong, J. M. White and M. Langell, *J. Vac. Sci. Technol., A*, 1997, **15**, 1146–1154.
22 T. D. Harris, D. H. Lee, M. Q. Blumberg and C. R. Arumainayagam, *J. Phys. Chem.*, 1995, **99**(23), 9530–9535.
23 X.-L. Zhou, P. M. Blass, B. E. Koel and J. M. White, *Surf. Sci.*, 1992, **271**(3), 427–451.
24 M. E. Castro, L. A. Pressley and J. M. White, *Surf. Sci.*, 1991, **256**, 227–241.
25 Y.-K. Kim, K. K. Irikura, M. E. Rudd, M. A. Ali, P. M. Stone, J. Chang, J. S. Coursey, R. A. Dragoset, A. R. Kishore and K. J. Olsen, *et al.*, *Electron-Impact Ionization Cross Section for Ionization and Excitation Database (version 3.0)*, National Institute of Standards and Technology, Gaithersburg, MD, 2004, available: http://physics.nist.gov/ionxsec [Friday, 31-Jan-2014 09:03:17 EST].
26 S. J. Garrett, D. V. Heyd and J. C. Polanyi, *J. Chem. Phys.*, 1997, **106**(18), 7834–7846.
27 E. Vichnevetski, P. Cloutier and L. Sanche, *J. Chem. Phys.*, 1999, **110**(16), 8112–8118.
28 S. E. Stein, *IR and Mass Spectra*. In NIST Chemistry WebBook, in *NIST Standard Reference Database Number 69*, ed. W. G. Mallard and P. J. Linstrom, National Institute of Standards and Technology, Gaithersburg, MD, 2000, 1,2-Ethanediol (http://webbook.nist.gov).
29 E. Illenberger and M. C. Meinke, *Int. J. Mass Spectrom.*, 2014, **365–366**, 80–85.
30 M. V. Muftakhof, R. F. Tuktarov and V. A. Mazunov, *Chem. Phys. Rep.*, 1999, **18**(3), 413–433.
31 B. Ómarsson, S. Engmann and O. Ingólfsson, *RSC Adv.*, 2014, **4**, 33222–33235.

Published on 14 November 2014. Downloaded by University of Groningen on 5/21/2019 9:45:41 AM.

32 J. K. Allen and J. C. Bevington, *Proc. R. Soc. A*, 1961, **262**(1309), 271–286.
33 Y. Watanabe, H. Ishigaki, H. Okada and S. Suyama, *Polym. J.*, 1997, **29**, 693–696.
34 (*a*) R. P. Bell, *Proc. R. Soc. A*, 1936, **154**(882), 414–429; (*b*) M. G. Evans and M. Polanyi, *Trans. Faraday Soc.*, 1938, **34**, 11–24.
35 (*a*) S. W. North, D. A. Blank, J. D. Gezelter, C. A. Longfellow and Y. T. Lee, *J. Chem. Phys.*, 1995, **102**(11), 4447–4460; (*b*) R. R. Lozada-García, J. Ceponkus, M. Chevalier, W. Chin, J.-M. Mestdaghd and C. Crépin, *Phys. Chem. Chem. Phys.*, 2012, **14**, 3450–3459.
36 E. Burean and P. Swiderek, *J. Phys. Chem. C*, 2008, **112**, 19456–19464.
37 M. Lepage, M. Michaud and L. Sanche, *J. Chem. Phys.*, 1997, **107**, 3478–3484.
38 F. W. McLafferty and F. Tureček, *Interpretation of mass spectra*, University Science Books, Sausalito, 1993, ISBN 0-935702-25-3.
39 B. C. Ibănescu and M. Allan, *Phys. Chem. Chem. Phys.*, 2009, **11**, 7640–7648.
40 S. Engmann, B. Ómarsson, M. Lacko, M. Stano, Š. Matejčík and O. Ingólfsson, *J. Chem. Phys.*, 2013, **138**, 234309.
41 J. Warneke, M. Lacko, P. Papp, M. Stano, Š. Matejčík and P. Swiderek, unpublished results.

 This journal is © the Owner Societies 2015